Front. Environ. Sci. Eng. 2013, 7(3): 420–427
DOI 10.1007/s11783-013-0489-0

RESEARCH ARTICLE

Chemical deactivation of V_2O_5-WO_3/TiO_2 SCR catalyst by combined effect of potassium and chloride

Xiaodong WU (✉)[1,2,3], Wenchao YU[1], Zhichun SI[2], Duan WENG[1,2]

1 State Key Laboratory of New Ceramics & Fine Process, Department of Materials Science and Engineering, Tsinghua University, Beijing 100084, China
2 Advanced Materials Institute, Graduate School at Shenzhen, Tsinghua University, Shenzhen 518055, China
3 Yangtze Delta Region Institute of Tsinghua University, Jiaxing 314000, China

Abstract V_2O_5-WO_3/TiO_2 catalyst was poisoned by impregnation with NH_4Cl, KOH and KCl solution, respectively. The catalysts were characterized by X-ray diffraction (XRD), inductively coupled plasma (ICP), N_2 physisorption, Raman, UV-vis, NH_3 adsorption, temperature-programmed reduction of hydrogen (H_2-TPR), temperature-programmed oxidation of ammonia (NH_3-TPO) and selective catalytic reduction of NO_x with ammonia (NH_3-SCR). The deactivation effects of poisoning agents follow the sequence of KCl > KOH ≫ NH_4Cl. The addition of ammonia chloride enlarges the pore size of the titania support, and promotes the formation of highly dispersed V = O vanadyl which improves the oxidation of ammonia and the high-temperature SCR activity. K^+ ions are suggested to interact with vanadium and tungsten species chemically, resulting in a poor redox property of catalyst. More importantly, potassium can reduce the Brønsted acidity of catalysts and decrease the stability of Brønsted acid sites significantly. The more severe deactivation of the KCl-treated catalyst can be mainly ascribed to the higher amount of potassium resided on catalyst.

Keywords V_2O_5-WO_3/TiO_2, potassium chloride, poisoning, reducibility, acid sites

1 Introduction

Nitrogen oxides (NO_x), emitted from automobile exhaust and power plant flue gas, can cause acid rain, photochemical smog and diseases of human respiratory system. The selective catalytic reduction (SCR) with ammonia has been proved to be an effective method for NO_x abatement [1]. Commercial V_2O_5-WO_3/TiO_2 NH_3-SCR catalyst, usually containing 0.5 wt.%–3 wt.% V_2O_5, 8 wt.%–10 wt.% WO_3 and TiO_2 as carrier [2,3]. V_2O_5 is considered as the main active component providing acid sites to adsorb and activate NH_3. WO_3 acts as an important promoter which favors the spreading of vanadia on the catalyst surface and stabilizes the anatase TiO_2 from phase transition to rutile. Furthermore, WO_3 increases the surface acidity of catalyst, and improves the poison resistance of catalyst to alkali metals [4].

Exhaust gases from stationary sources such as power plant always contain alkali oxides and salts which could strongly poison the catalyst. Among the alkali metals, potassium is the most serious poison for vanadium-based catalysts. Therefore, the deactivation effect of alkali metals especially potassium have been widely studied. Alkali can combine with dispersed vanadium species and neutralize the Brønsted acid sites, leading to the decrease of SCR activity [5–8]. The poisoning of V_2O_5-WO_3/TiO_2 catalyst by alkali hydroxides and nitrates has been studied by some researchers, but alkali metal compounds in the real exhaust gas from stationary sources are always in the form of more stable ones such as chloride and sulfate. A few of studies have been carried out to explore the poisoning mechanisms of KCl on V_2O_5-WO_3/TiO_2 catalyst. Lisi et al. [9] observed a decrease of vanadium content of catalyst under an HCl-containing gas flow, and suggested the replacement of original acid site by the formation of new acid sites provided by HCl, which showed a lower activity. Jensen's group [10] reported that potassium salts in the form of chlorides and sulfates are strong poisons for SCR catalyst by neutralizing the active sites for NH_3 adsorption and SCR reaction. Their further studies showed that, in addition to the main cause of deactivation by chemical poisoning of active sites, physical blocking of the outer wall surface also contributes to the loss of activity of

Received October 18, 2012; accepted December 15, 2012

E-mail: wuxiaodong@tsinghua.edu.cn

monolithic catalyst in practical applications [11,13]. Although the effects of potassium chloride on the surface acidity and SCR activity of catalysts have been studied, the attention paid to the changes of structural and redox properties of catalyst induced by potassium chloride is not enough.

In this work, the deactivation of the homemade V_2O_5-WO_3/TiO_2 SCR catalyst by potassium chloride was explored. The structural and textural properties of the catalysts were characterized by XRD, ICP, N_2 physisorption, Raman, UV-vis. FT-IR of NH_3 adsorption, H_2-TPR and NH_3 oxidation measurements were carried out to evaluate the surface acidity and redox properties of the catalysts, respectively. The single and combined effects of potassium and chloride on the catalytic behavior of V_2O_5-WO_3/TiO_2 catalyst were clarified.

2 Experimental

2.1 Preparation of the catalysts

The V_2O_5-WO_3/TiO_2 (VWT) catalyst was prepared by a two-step impregnation method. Nano TiO_2 powders (Millennium DT-51) were mixed with ammonium paratungstate solution by magnetic stirring for 1 h. The obtained mixture was dried at 110°C overnight and calcined at 450°C for 4 h in air to obtain WO_3/TiO_2 powders. Then, a solution of ammonium metavanadate and oxalic acid was impregnated. The obtained paste was dried at 110°C overnight and calcined at 450°C for 4 h. The nominal weight ratio of V_2O_5:WO_3:TiO_2 in the catalyst was 1:10:90.

The potassium poisoned samples were prepared by impregnating excess water solution of KOH or KCl onto the obtained V_2O_5-WO_3/TiO_2 powders with a nominal weight ratio 1 wt.% of K_2O, denoted as VWT(KOH) and VWT(KCl), respectively. The impregnated powders were then dried overnight and calcined at 400°C for 2 h. For reference, a sample VWT(NH_4Cl) with a theoretical weight ratio 1 wt.% of NH_4Cl was prepared with the same process.

2.2 Catalyst characterization

The powder X–ray diffraction (XRD) patterns were determined by a diffractometer (D8 ADVANCE, Bruker, Germany) employing Cu Kα radiation (λ = 0.15418 nm) operating at 40 kV and 30 mA.

The inductively coupled plasma (ICP) analysis was carried out using an ICP emission spectrometer (Vista-MPX, Varian, America).

Textural properties were determined by nitrogen physisorption at −196°C using a JW–BK122F (Beijing JWGB, China) instrument. Prior to nitrogen physisorption measurement, the samples were degassed to 0.01 Pa at 220°C. The specific desorption pore volume was assessed by the Barrett–Joyner–Halenda (BJH) method.

The Raman spectra were obtained at ambient condition on a confocal micro–Raman apparatus (Aurora J300, IDSpec, China) using Ar^+ laser with a CCD detector. Pure powder supported on a sheet glass was used without any pretreatment. The laser wavelength was 632.8 nm and the exposure time was 20 s.

The ultraviolet-visible (UV-vis) absorption spectroscopy was measured by using an UV-vis spectrophotometer (Hitachi U-3010) equipped with an integrating sphere. A $BaSO_4$ pellet was used as a reference. The spectra were recorded at room temperature (RT) in the spectral range 200 nm–800 nm.

The *in-situ* infrared (IR) spectra of ammonia adsorption were recorded on a FT-IR spectrometer (Nicolet 6700, Thermo Fisher, America) equipped with a MCT detector. The catalyst was pretreated in 20% O_2/N_2 flow (100 $mL{\cdot}min^{-1}$) at 450°C for 30 min, and then saturated with ammonia (1000 ppm NH_3/N_2, 100 $mL{\cdot}min^{-1}$) for 30 min. After purging with N_2 for 30 min at different temperatures (RT and 200°C), the spectra were collected by accumulating 32 scans at a resolution of 4 cm^{-1}.

H_2 temperature-programmed reduction (H_2-TPR) was conducted on a chemical adsorption instrument (AutoChem II 2920, Micromeritics, America). Prior to the test, 50 mg of sample was purged in He (50 $mL{\cdot}min^{-1}$) at 450°C for 30 min, then cooled down to room temperature. The reactor temperature was raised to 900°C at a constant heating rate of 10°C min^{-1} in 10% H_2/Ar with a flow rate of 50 $mL{\cdot}min^{-1}$.

2.3 Activity measurement

The NH_3-SCR activity measurement was carried out in a fixed bed reactor with 200 mg catalyst (diluted to 1 mL with silica pellets). The reaction gas mixture consisted of 500 ppm NO, 500 ppm NH_3, 5% O_2 and N_2 in balance. Prior to the measurement, the catalysts were treated in 20% O_2/N_2 at 450°C for 30 min. The measurement was performed at fixed temperatures per 50°C from 150 to 450°C and kept for 20 min at each point. The gas hourly space velocity (GHSV) was 30000 h^{-1}. The feed and product concentrations were measured by Nicolet 380 at 120°C. The NH_3-SCR activity of catalysts was shown as NO_x (NO, NO_2 and N_2O) conversions which were calculated as follows:

$$NO_x \text{ conversion } (\%) = \frac{[NO]_{in} - [NO]_{out} - [NO_2]_{out} - 2[N_2O]_{out}}{[NO]_{in}} \times 100, \quad (1)$$

NH_3 oxidation experiments were performed by the similar conditions in SCR reaction in which NO in gas

mixture was excluded. NH_3 conversion was defined by Eq. (2).

$$NH_3 \text{ conversion } (\%) = \frac{[NH_3]_{in} - [NH_3]_{out}}{[NH_3]_{in}} \times 100, \quad (2)$$

The first-order rate constant was calculated according to Eq. (3),

$$k = \frac{F_0}{[NO]_{in} W} \ln(1 - X). \quad (3)$$

where W was the weight of the catalyst, F_0 was the inlet molar flow rate of nitric oxide, $[NO]_{in}$ was the inlet molar concentration, and X was the conversion of nitric oxide [4]. The reaction was performed at fixed temperatures with 10 mg of catalyst (diluted with 90 mg of silica pellets) and the gas concentration was the same as above. The total flow rate was enhanced to 1 L·min^{-1} to reach a high GHSV of 750000 h^{-1}.

3 Results and discussion

3.1 NH_3-SCR activities

Figure 1 shows the de-NO_x activities of the fresh and poisoned V_2O_5-WO_3/TiO_2 catalysts. The fresh catalyst achieves above 80% NO_x conversion in the temperature range 240°C–450°C and reaches nearly 100% conversion at 300°C–400°C. The poisoning effects of different agents follow the order of KCl > KOH ≫ NH_4Cl. The catalyst is severely deactivated by potassium chloride with only about 35% of the original NO_x conversion values achieved at 300°C–400°C. A moderate deactivation of catalyst is attained by KOH with a maximal NO_x conversion of about 65% at 300°C–350°C. Contrarily, the activity of the catalyst remains high after the impregnation of NH_4Cl, with only an abnormal data decreasing from 89% to 75% at 250°C. Thus, the chloride itself leads to almost no deactivation of V_2O_5-WO_3/TO_2 catalyst, but the impregnation of potassium chloride results in a more severe deactivation of the catalyst than the KOH poisoning. Almost no NO_2 is observed in the downstream during the whole temperature region, and only less than 15 ppm of N_2O is generated at high temperatures, indicating a high selectivity to N_2 (always > 95%) for all the catalysts.

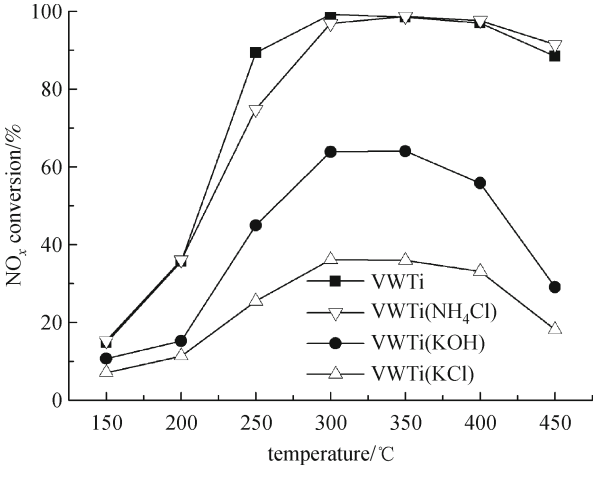

Fig. 1 NH_3-SCR activities of the catalysts

To compare the level of deactivation quantitatively, the first-order rate constant was measured under higher space velocity and the results are shown in Fig. 2. A similar tendency of catalytic activity for different catalysts is observed. The fresh catalyst shows higher activity than the poisoned catalysts at low temperatures such as 250°C. The poisoning effect of potassium is significant for VWT (KOH) and especially VWT(KCl) catalysts. Again, slightly higher catalytic activities of the catalyst impregnated with NH_4Cl are observed at 300°C and 350°C compared with the fresh sample.

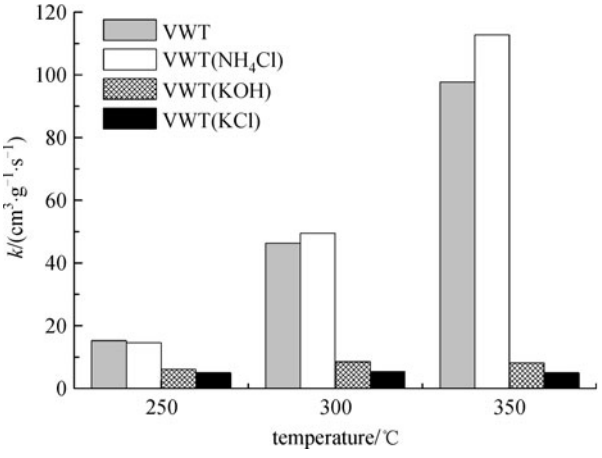

Fig. 2 The first-order rate constants for NO reduction

3.2 Solid properties

Figure 3 shows the XRD patterns of the catalysts. All the samples exhibit only the characteristic peaks of anatase titania. The absence of diffraction peaks of WO_3 and V_2O_5 indicates the formation of uniformly spread oxotungsten and amorphous state of vanadia. Meanwhile, no detectable formation of potassium salts or chlorides occurs.

Both potassium and chloride are easy to loss during the preparation process due to their high volatility. To detect the residual contents of potassium and chloride in the poisoned catalysts, the ICP measurement was performed and the results are listed in Table 1. The measured potassium contents are lower than the nominal metal content (0.83 wt.%), which cannot be ascribed to the volatility of potassium since no obvious variations were detected for VWT(KOH) and VWT(KCl) catalysts before and after the calcination. Such a phenomenon usually occurs when catalysts are prepared by excess solution

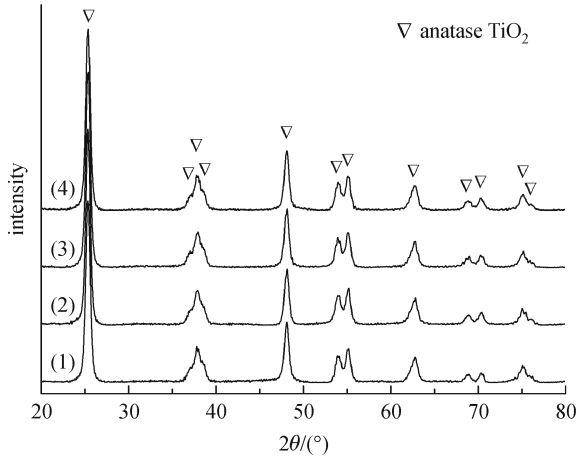

Fig. 3 XRD patterns of (1) VWT, (2) VWT(NH_4Cl), (3) VWT(KOH) and (4) VWT(KCl) catalysts

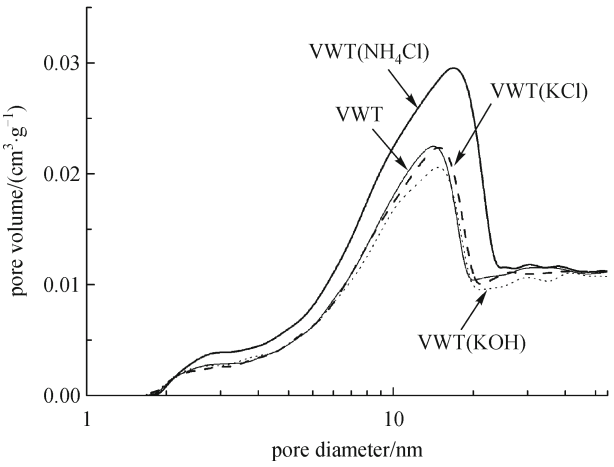

Fig. 4 Pore size distributions of the catalysts

impregnation [13]. It is also observed by Tikhomirov et al. who ascribed the lower fraction of potassium in the final catalyst to an incomplete impregnation process, as part of the potassium nitrate was forming separate crystallites instead of depositing on the metal oxide surface [14]. The residual contents of chloride are even much lower due to its extra high volatility. It is noted that the potassium content in VWT(KCl) is higher than that in VWT(KOH), which may be related to the more homogeneous distribution of potassium chloride.

Figure 4 shows the pore size distributions of the catalysts. All the catalysts yield a pore diameter distribution centered at 11.5 nm, which is mainly assigned to the pore structure of the titania support. The impregnation of NH_4Cl increases the pore volume to some extent due to the corrosion effect of chloride. Pore size distribution confirms that no significant pore blocking occurs upon potassium deposition. Consequently, a negligible effect of poisoning agents on the surface area of the samples is observed (Table 1). The changes of surface area and pore volume do not seem to explain the severe decrease in the activity of the K-poisoned catalysts.

3.3 Raman and UV-vis spectra

It is generally accepted that potassium exists in the form of vanadate on the poisoned SCR catalyst although few evidences have been presented [5]. Figure 5 shows the Raman spectra in the range 1100–800 cm^{-1} under ambient conditions, which provide some evidences for the existence of potassium vanadate. A broad band at 986 cm^{-1} is assigned to the symmetric V = O stretching mode of two dimensional surface vanadium species. The Raman band of tungsten oxide species is not observed because of their lower intensity compared to that of V = O groups. With the introduction of potassium, this band shifts slightly toward lower wavenumbers (980 cm^{-1}), suggesting that potassium changes the surface vanadia species from decavanadate to metavanadate form due to its basic nature [8]. An intense band appears at 968 cm^{-1} for the KOH- and especially KCl-poisoned catalysts. It is assigned to highly dispersed potassium vanadate, KVO_3, which appears at 946 cm^{-1} in the crystalline phase as reported [8]. Contrarily, the Raman band related to V = O groups shifts toward 990 cm^{-1} for the ammonia chloride-treated sample, implying the inverse change of the structure of surface VO_x species from metavanadate to decavanadate.

To further elucidate the chemical interactions between the poisoning agents and vanadia, the UV-vis spectra of the fresh and poisoned catalysts are shown in Fig. 6. The spectra are dominated by the edge relative to the $O^{2-} \rightarrow Ti^{4+}$ charge transfer of the anatase support at 380 nm [15]. A broad absorption edge in the range 450–550 nm is sensitive to the coordination structure of vanadia, and that

Table 1 Structural and textural properties of the catalysts

catalysts	ICP		$S_{BET}/(m^2 \cdot g^{-1})$	$V_P/(cm^3 \cdot g^{-1})$
	K^+/wt.%	Cl^-/wt.%		
VWT	–	–	76	0.289
VWT(NH_4Cl)	–	0.003	78	0.302
VWT(KOH)	0.58	–	77	0.270
VWT(KCl)	0.66	0.014	77	0.274

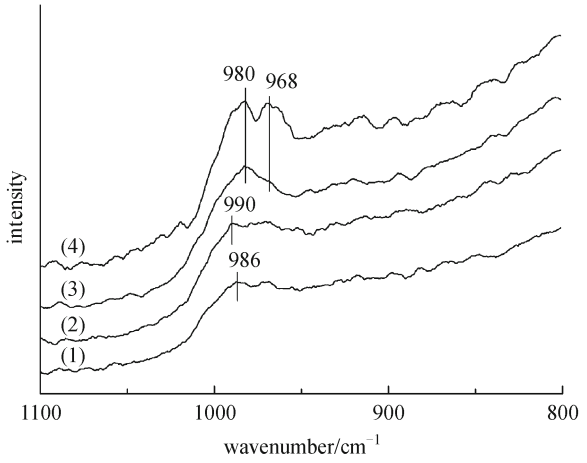

Fig. 5 Raman spectra of (1) VWT, (2) VWT(NH_4Cl), (3) VWT (KOH) and (4) VWT(KCl) catalysts

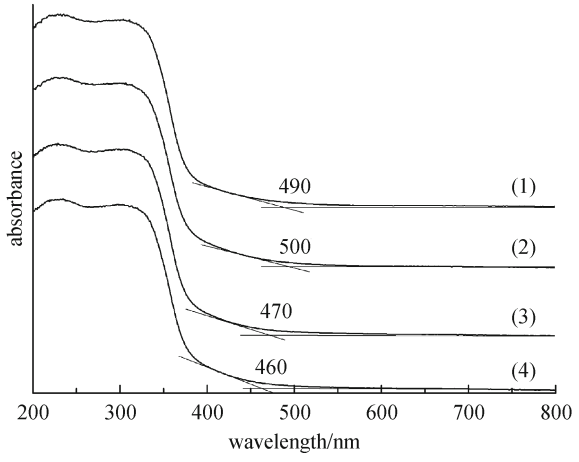

Fig. 6 UV-vis spectra of (1) VWT, (2) VWT(NH_4Cl), (3) VWT (KOH) and (4) VWT(KCl) catalysts

the higher the absorption edge wavelength, the higher the coordination of polymeric vanadia species [7]. In this case, the absorption edge position increases from 490 nm to 500 nm when impregnation NH_4Cl onto the catalyst, suggesting that the formation of vanadium chloride and the volatilization of Cl^- ions result in the redispersion of vanadia and an increase of their polymerization degree, leading to a higher reducibility. In comparison, the absorption edge position decreases to 470 nm with the impregnation of KOH, implying that K^+ ions combine strongly with dispersed vanadia species. This trend is more obvious for the VWT(KCl) catalyst with the absorption edge position shift to lower wavelengths (460 nm), which may be related to the larger amount of potassium vanadate produced and is consistent with the Raman result.

3.4 NH_3 adsorption

It has been established that the surface acidity of V_2O_5-WO_3/TiO_2 catalyst plays an important role in the selective reduction of NO_x by NH_3. To investigate the influences of potassium and chloride on the acid sites of the catalysts, the IR spectra in the ranges of 1800–1200 cm^{-1} obtained after NH_3 adsorption at room temperature and 200°C are shown in Fig. 7. The IR spectra of the fresh V_2O_5-WO_3/TiO_2 catalyst shows the presence of the ammonia species coordinated on Lewis acid sites (1602 cm^{-1}, $\delta_{as}NH_3$; 1238–1220 cm^{-1}, δ_sNH_3), ammonium ions coordinated to Brønsted acid sites (1675 cm^{-1}, $\delta_sNH_4^+$; 1440 cm^{-1}, $\delta_{as}NH_4^+$) [16]. Clearly, ammonia adsorbed on Brønsted acid sites is more predominant than that adsorbed on Lewis acid sites. Activation of ammonia would occur on the surface Brønsted acid sites. On the other hand, the weak bands at 1560 cm^{-1} and 1346–1320 cm^{-1} are assigned to NH_2 scissoring and NH_2 wagging of N_2H_4 species, respectively. It means that dehydrogenation of NH_3 to NH_2 also occurs on the surface of V_2O_5-WO_3/TiO_2 catalyst even at room temperature. However, the amide species are not observed on the potassium-poisoned catalysts.

It can be seen that the ammonia chemisorption at room temperature is strongly suppressed on the potassium-poisoned catalysts, and the adsorbed ammonia species are very unstable. As shown in Fig. 7(b), the bands associated with Lewis acid sites (1607 cm^{-1}, 1324 cm^{-1} and 1238 cm^{-1}) become much weaker on VWT(KOH) and VWT(KCl) catalysts at 200°C, and those related to Brønsted acid sites (1672 cm^{-1} and 1420 cm^{-1}) decrease even more sharply. The important first step for SCR reaction is chemisorption of NH_3 on the Brønsted acid site V–OH. Based on the Raman and UV-vis results, potassium can combine with surface vanadia, resulting in a substantial decrease in the ammonia adsorption. The band at 1420 cm^{-1} on VWT(KCl) is weaker than that on VWT(KOH), implying that more Brønsted acid sites are neutralized. On the other hand, both the adsorption of ammonia and the stability of the adsorbed ammonia species appear to be little affected by impregnation of ammonia chloride.

3.5 Redox property

Figure 8 shows the H_2-TPR profiles of the catalysts. The fresh V_2O_5-WO_3/TiO_2 catalyst shows two reduction peaks at 478°C and 769°C, corresponding to the reduction of $V^{5+} \rightarrow V^{3+}$ and $W^{6+} \rightarrow W^0$ which are promoted by strong interaction with TiO_2 support, respectively [6,17]. The low-temperature reduction peak shifts to 380°C for the VWT(NH_4Cl) catalyst which can be explained by the fact that vanadate species are easily reacting with ammonia chloride to form soluble vanadium chloride. Gazzoli *et al.*

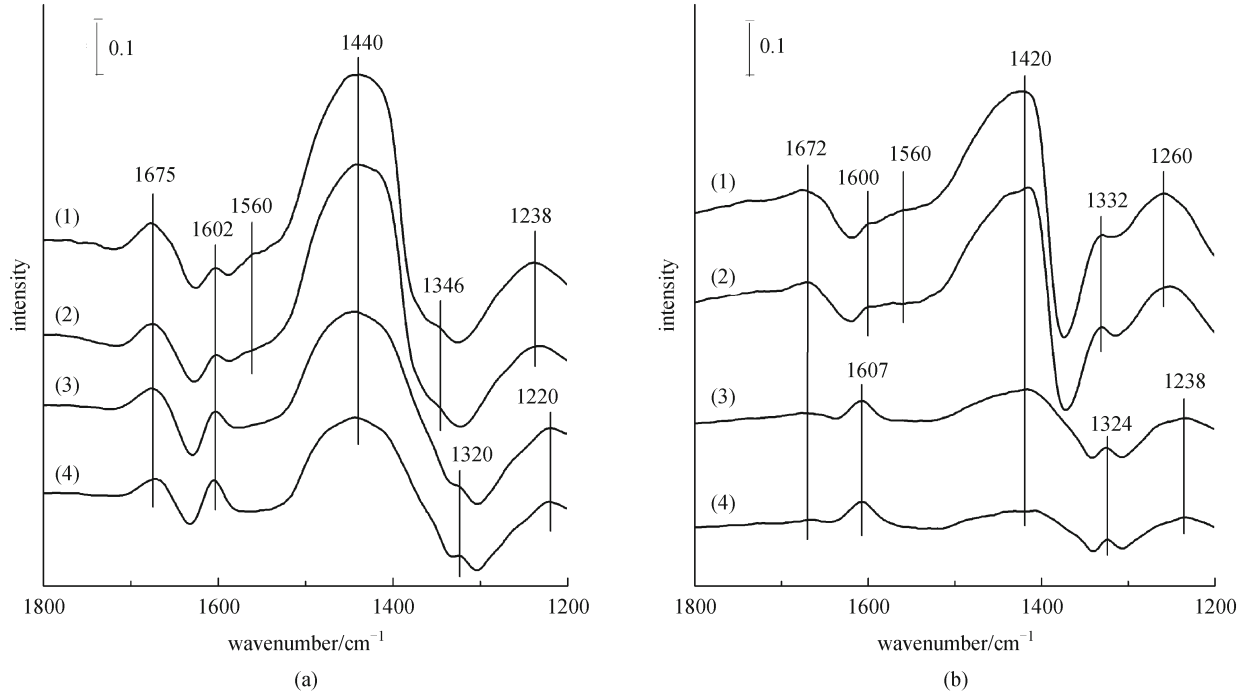

Fig. 7 FTIR spectra of (1) VWT, (2) VWT(NH_4Cl), (3) VWT(KOH) and (4) VWT (KCl) catalysts arising from contact of NH_3 at (a) room temperature and (b) 200°C

[18] assigned the hydrogen consumption in the range 303°C–343°C to small polymeric VO_x anchored to the zirconia surface and in the range 403°C–453°C to larger polymeric aggregates for V_2O_5/ZrO_2 catalyst after leaching with an ammonia solution. Similarly, the shift of the reduction peak toward lower temperatures in our case can be also ascribed to the formation of polymeric VO_x species anchored to the titania surface, which is more reducible. Contrarily, the reducibility of vanadia is weakened by the impregnation of potassium hydroxide with the low-temperature reduction peak shifting to 497°C for VWT (KOH), implying the formation of less active vanadate species such as KVO_3 [19]. The reducibility of tungsten oxide appears to be improved for both VWT(NH_4Cl) and VWT(KOH) catalysts, which is probably due to the chemical transformation of WO_3 to more active WO_4^{2-} species and further polytungstate [20]. A similar promotion effect of potassium addition on the onset temperature of the reduction of WO_3 has been reported for WO_3/SiO_2 catalyst [21]. However, WO_x species are suggested to contribute little to the low-temperature redox property of the catalyst since its reduction temperature is much higher than that of VO_x.

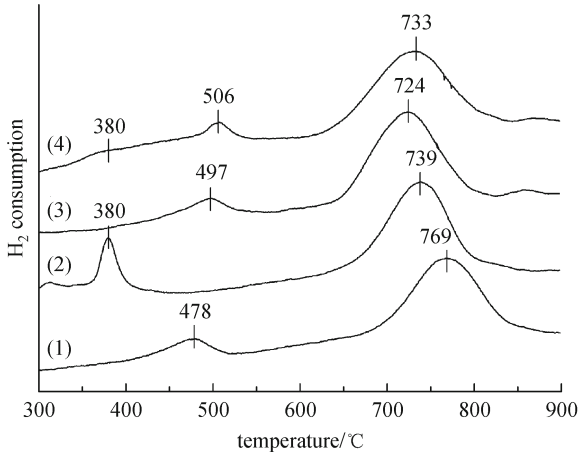

Fig. 8 H_2-TPR curves of (1) fresh, (2) VWT(NH_4Cl), (3) VWT (KOH) and (4) VWT(KCl) catalysts

The TPR curve of VWT(KCl) catalyst represents three reduction peaks. The first reduction peak at 380°C becomes much weaker and the second one shifts to 506°C. So there are at least two forms of vanadia, i.e., highly dispersed and aggregated species. In respect to NH_4Cl, the relatively stable potassium chloride reduces the availability of free chloride ions which act as the promoter for the redispersion of vanadia during the impregnation procedure, and the formation of O = V-OHCl groups would be replaced by the alkali metal doped during the drying and calcination processes [17]. Thus, the first reduction peak decreases sharply in intensity. Meanwhile, the formation of more potassium vanadate causes the shift of the second reduction peak to higher temperature.

3.6 NH_3 oxidation

Figure 9 shows the NH_3-TPO curves of the V_2O_5-WO_3/TiO_2 catalysts. The onset of ammonia catalytic oxidation

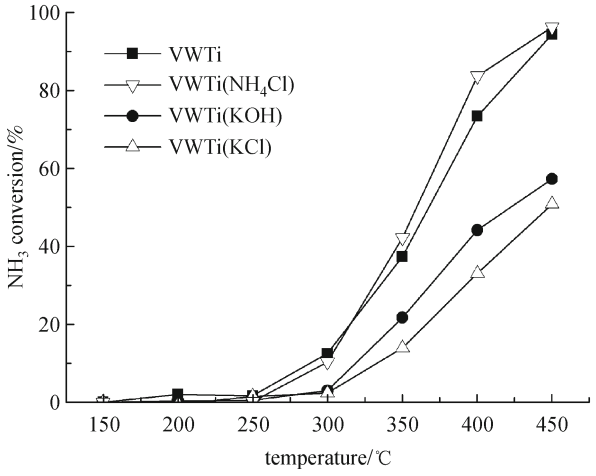

Fig. 9 NH_3 oxidation curves of the catalysts

occurs at 250°C over the fresh catalyst, and the ammonia conversion reaches 94% at 450°C. The VWT(NH_4Cl) catalyst exhibits a slightly higher activity for ammonia oxidation and the potassium-poisoned catalysts show worsened catalytic activities, which correlates well with their redox properties. Generally, the high activity of the catalyst for competitive ammonia oxidation at high temperatures will lead to a low NO_x conversion due to the lack of the reductant. However, it does not conform to the V_2O_5-WO_3/TiO_2 catalysts investigated here. It is suggested that a key step in the SCR reaction is the activation of the adsorbed ammonia species, i.e., ammonia protonation to ammonium ions on Brønsted acid sites, and hydrogen abstracting of ammonia coordinated on Lewis acid sites to a less important degree. It depends strongly on the acidic properties of the catalysts and is severely suppressed by the addition of potassium.

4 Conclusions

The deactivation effects of NH_4Cl, KOH and KCl on the NH_3-SCR activity of V_2O_5-WO_3/TiO_2 catalyst were investigated. The changes of physical properties such as surface area and pore structure can be excluded responsible for the severe deactivation of the potassium-poisoned catalysts. The activation of the adsorbed ammonia species, which depends strongly on the acidic property of the catalysts, is suggested to be a key step in the SCR reaction. The impregnation with potassium chloride results in the formation of less active potassium vanadate instead of the redispersion of more active vanadia in the case of the treatment with ammonia chloride. More importantly, the chemical combination of potassium with vanadia and tungsten oxides decreases the amount and stability of ammonium ions coordinated on Brønsted acid sites. The deactivation of the catalyst depends strongly on the amount of potassium, and the role of anionic species is much less important.

Acknowledgements The authors would like to acknowledge the financial support from Shenhua Group Corporation Limited and Science and Technology Department of Zhejiang Province Project 2011C31010.

References

1. Busca G, Lietti L, Ramis G, Berti F. Chemical and mechanistic aspects of the selective catalytic reduction of NO_x by ammonia over oxide catalysts: a review. Applied Catalysis B: Environmental, 1998, 18(1–2): 1–36
2. Alemany L J, Lietti L, Ferlazzo N, Forzatti P, Busca G, Giamello E, Bregani F. Reactivity and physicochemical characterization of V_2O_5-WO_3/TiO_2 de-NO_x catalysts. Journal of Catalysis, 1995, 155 (1): 117–130
3. Shi A J, Wang X Q, Yu T, Shen M Q. The effect of zirconia additive on the activity and structure stability of V_2O_5/WO_3-TiO_2 ammonia SCR catalysts. Applied Catalysis B: Environmental, 2011, 106(3–4): 359–369
4. Chen J P, Yang R T. Role of WO_3 in mixed V_2O_5-WO_3/TiO_2 catalysts for selective catalytic reduction of nitric oxide with ammonia. Applied Catalysis A: General, 1992, 80(1): 135–148
5. Kröcher O, Elsener M. Chemical deactivation of V_2O_5/WO_3-TiO_2 SCR catalysts by additives and impurities from fuels, lubrication oils, and urea solution I. Catalytic studies. Applied Catalysis B: Environmental, 2007, 75: 241–253
6. Chen L, Li J H, Ge M F. The poisoning effect of alkali metals doping over nano V_2O_5-WO_3/TiO_2 catalysts on selective catalytic reduction of NO_x by NH_3. Chemical Engineering Journal, 2011, 170 (2–3): 531–537
7. Tang F S, Xu B L, Shi H H, Qiu J H, Fan Y N. The poisoning effect of Na^+ and Ca^{2+} ions doped on the V_2O_5/TiO_2 catalysts for selective catalytic reduction of NO by NH_3. Applied Catalysis B: Environmental, 2010, 94(1–2): 71–76
8. Kamata H, Takahashi K, Odenbrand C H I. The role of K_2O in the selective reduction of NO with NH_3 over a $V_2O_5(WO_3)/TiO_2$ commercial selective catalytic reduction catalyst. Journal of Molecular Catalysis A: Chemical, 1999, 139(2–3): 189–198
9. Lisi L, Lasorella G, Malloggi S, Russo G. Single and combined deactivating effect of alkali metals and HCl on commercial SCR catalysts. Applied Catalysis B: Environmental, 2004, 50(4): 251–258
10. Zheng Y J, Jensen A D, Johnsson J E. Laboratory investigation of selective catalytic reduction catalysts: deactivation by potassium compounds and catalyst regeneration. Industrial & Engineering Chemistry Research, 2004, 43(4): 941–947
11. Zheng Y J, Jensen A D, Johnsson J E, Thøgersen J R. Deactivation of V_2O_5-WO_3-TiO_2 SCR catalyst at biomass fired power plants: elucidation of mechanisms by lab- and pilot-scale experiments. Applied Catalysis B: Environmental, 2008, 83(3–4): 186–194
12. Putluru S S R, Jensen A D, Riisager A, Fehrmann R. Alkali resistivity of Cu based selective catalytic reduction catalysts:

potassium chloride aerosol exposure and activity measurements. Catalysis Communications, 2012, 18: 41–46

13. San José-Alonso D, Illán-Gómez M J, Román-Martínez M C. K and Sr promoted Co alumina supported catalysts for the CO_2 reforming of methane. Catalysis Today, 2011, 176(1): 187–190
14. Tikhomirov K, Kröcher O, Wokaun A. Influence of potassium doping on the activity and the sulfur poisoning resistance of soot oxidation catalysts. Catalysis Letters, 2006, 109(1–2): 49–53
15. Larrubia M A, Busca G. An ultraviolet–visible–near infrared study of the electronic structure of oxide-supported vanadia–tungsta and vanadia–molybdena. Materials Chemistry and Physics, 2001, 72(3): 337–346
16. Ramis G, Yi L, Busca G. Ammonia activation over catalysts for the selective catalytic reduction of NO_x and the selective catalytic oxidation of NH_3: an FT-IR study. Catalysis Today, 1996, 28(4): 373–380
17. Wan Q, Duan L, Li J H, Chen L, He K B, Hao J M. Deactivation performance and mechanism of alkali (earth) metals on V_2O_5-WO_3/TiO_2 catalyst for oxidation of gaseous elemental mercury in simulated coal-fired flue gas. Catalysis Today, 2011, 175(1): 189–195
18. Gazzoli D, De Rossi S, Ferraris G, Mattei G, Spinicci R, Valigi M. Bulk and surface structures of V_2O_5/ZrO_2 catalysts for *n*-butane oxidative dehydrogenation. Journal of Molecular Catalysis A: Chemical, 2009, 310(1–2): 17–23
19. Bulushev D A, Rainone F, Kiwi-Minsker L, Renken A. Influence of potassium doping on the formation of vanadia species in V/Ti oxide catalysts. Langmuir, 2001, 17(17): 5276–5282
20. Huang S J, Liu S L, Zhu Q J, Zhu X X, Xin W J, Liu H J, Feng Z C, Li C, Xie S J, Wang Q X, Xu L Y. The effect of calcination time on the activity of WO_3/Al_2O_3/HY catalysts for the metathesis reaction between ethene and 2-butene. Applied Catalysis A: General, 2007, 323: 94–103
21. Erdőhelyi A, Németh R, Hancz A, Oszkó A. Partial oxidation of methane on potassium-promoted WO_3/SiO_2 and on K_2WO_4/SiO_2 catalysts. Applied Catalysis A: General, 2001, 211(1): 109–121